Unsteady Propeller–Wing Interaction at Varying Propeller Tilt Angles: A Blade–Resolved URANS Study

Talenta Unggul 3P

Mochammad Agoes Moelyadi[1], Muhammad Farras Arira[1], Rizky Amalis Zhuraida[1]

[1] Pusat Studi Sistem Tak Berawak, Institut Teknologi Bandung

Abstract

Tilting propellers are central to many vertical take-off and landing configurations, yet studies of tilted propeller–wing systems have reported mainly time-averaged loads. This paper quantifies how the mean and blade-passing propeller–wing interaction changes with tilt. Blade-resolved, sliding-mesh URANS simulations with the k–ω SST model were performed for a four-bladed propeller (J = 0.8, Re_D = 6.4×10^5) at mid-semispan ahead of a straight wing at zero incidence, pivoted about the wing leading edge to 0°, 30° and 45°.

The integral loads change by less than 0.5% between the medium and fine meshes, and the isolated-propeller thrust is within 4.4% of the measurement at J = 0.8. Tilting to 45° at constant rotational speed raises the thrust coefficient by 89%, lowers the efficiency from 0.72 to 0.65 and makes each blade's thrust vary by 77% once per revolution. The wing changes from a small net lift to a download that cancels 27% of the vertical propeller force. The pitching moment is non-monotonic, with a nose-down extremum at 30° four times larger than at 45°. Pressure cuts and phase-locked flow fields show that it arises when the wing leading edge lies in the lower shear layer of the deflected slipstream, where a lower-surface suction peak and tip vortices travelling along the lower surface produce a nose-down couple with little net lift. The blade-passing lift amplitude grows 16-fold with tilt. The trim moment during transition is thus largest at intermediate tilt.

Keyword: Propeller-wing interaction, Tilting propeller, Unsteady RANS

Introduction

Electric and hybrid-electric propulsion have renewed interest in VTOL aircraft with tilting propellers, enabling vertical take-off and landing and efficient wing-borne cruise. During flight transition, propeller tilt changes the inflow conditions and deflects the slipstream relative to the wing, resulting in complex aerodynamic interactions that influence aircraft performance and stability.

Previous experimental and numerical studies have primarily investigated time-averaged aerodynamic characteristics of tilted propeller–wing configurations. However, the blade-resolved unsteady loading, spatial distribution of wing pressure fluctuations, and underlying vortex dynamics remain insufficiently understood, particularly for mid-span-mounted propellers.

This study investigates the unsteady propeller–wing interaction at different propeller tilt angles using blade-resolved, sliding-mesh URANS simulations. The effects of tilt angle on aerodynamic performance, blade-passing harmonics, unsteady wing loading, and slipstream–wing vortex interactions are examined.

Research Method

The URANS simulations were performed using the pressure-based coupled solver in ANSYS Fluent 2026 R1, with the computational geometry and boundary conditions shown in Figures 1 and 2.

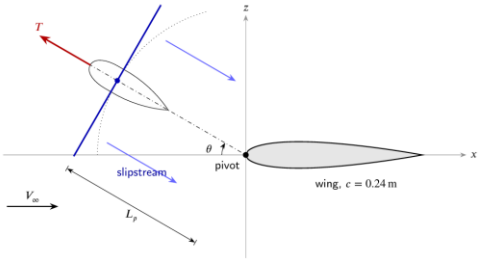


Figure 1. Side view of the tilt kinematics for θ = 30°

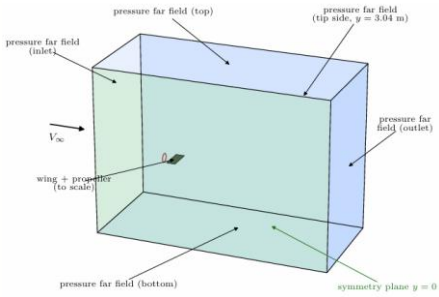


Figure 2. Boundary conditions

Simulations were conducted at 40 m/s and 1326 rad/s for tilt angles of 0°, 30°, and 45°, using a time step of 2.6325 × 10^{-5} s (2° rotation) and eight iterations per step. Data were sampled over three revolutions using a 24.6-million-cell mesh with (y^+< 1) on over 99.8% of blade and wing surfaces.

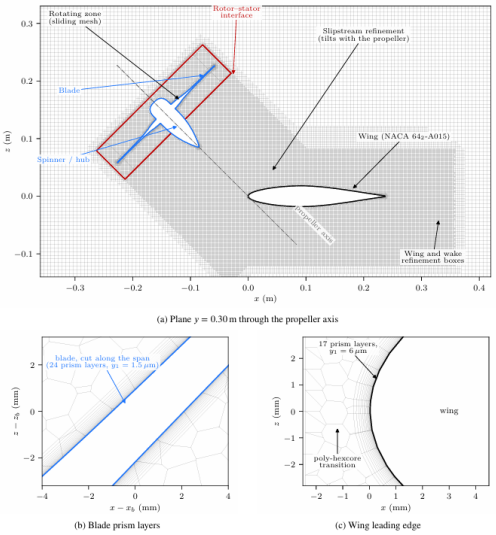


Figure 3. Computational mesh at θ = 45°

Aerodynamic performance was evaluated using propeller thrust, power, efficiency, in-plane forces, and wing lift, drag, and pitching moment coefficients. Unsteady loading was analysed through Fourier spectral analysis, blade-passing harmonics, and RMS surface pressure. Phase-averaged flow fields and Q-criterion visualisations were used to examine slipstream–wing interactions and vortex dynamics at different propeller tilt angles.

Discussion & Result

The 4P wing-lift amplitude increased from 2.3 × 10^{-4} at 0° to 2.1 × 10^{-3} at 30° and 3.8 × 10^{-3} at 45° (≈16 times). At 45°, the 8P harmonic reached 19% of the 4P amplitude, while broadband fluctuations accounted for 55% of the lift-fluctuation energy, indicating stronger, more impulsive loading and spinner–hub wake interaction with the wing.

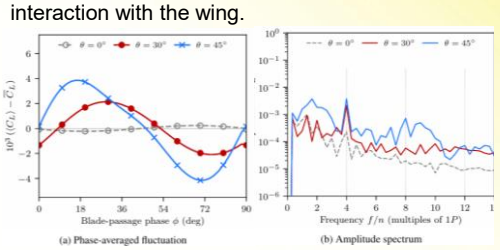


Figure 4. Unsteady wing lift versus tilt angle

Table 1. Time-averaged wing loads vs. tilt angle

θ (deg)	$\overline{C_L}$	$\overline{C_D}$	$\overline{C_{L,\mathrm{strip}}}$	$10^3\,C_L$ RMS	$10^3\,C_L$ peak-to-peak
0	0.0020 ± 0.0002	0.0117	0.0008	1.04	4.20
30	−0.0039 ± 0.0007	0.0123	−0.0126	1.85	8.48
45	−0.0398 ± 0.0008	0.0111	−0.0402	4.90	19.88

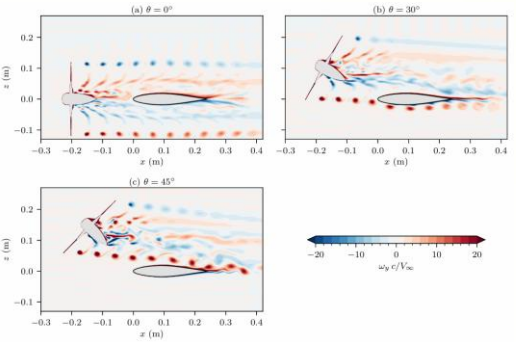


Figure 5. Instantaneous spanwise vorticity at y = 0.30m and ϕ = 0°

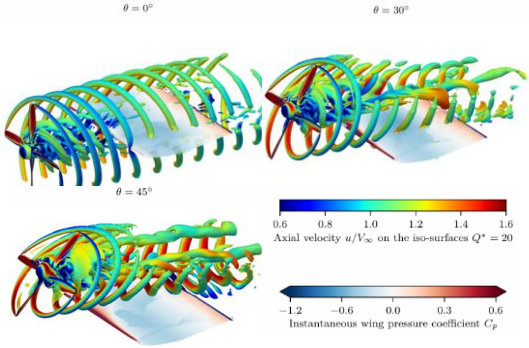


Figure 6. Instantaneous vortical structures at blade-passage phase ϕ = 0°

Conclusion

Thrust increased by 89% from 0° to 45°, while efficiency dropped from 0.716 to 0.645. Wing lift changed from (C_L=0.002) at 0° to a download, cancelling 4% and 27% of vertical propeller force at 30° and 45°. Blade-passing lift amplitude increased 16-fold, with broadband fluctuations contributing 55% of the energy at 45°. The strongest nose-down moment occurred at 30° (C_M=-0.0104), with the effective load position shifting to (x/c=0.43).